THE MID-INFRARED SPATIALLY RESOLVED ENVIRONMENT AROUND R CRA. H. Zinnecker, S. Correia, G. Meeus, *Astrophysikalisches Institut Potsdam, An der Sternwarte 16, D-14482 Potsdam, Germany, scorreia@aip.de, gwen@aip.de, hzinnecker@aip.de*, R. Lachaume, *Max-Planck-Institut für Radioastronomie, auf dem Hügel 69, D-53121 Bonn, Germany, lachaume@mpifr-bonn.mpg.de*, R. Köhler, *Sterrewacht Leiden, Niels Bohrweg 2, NL-2333 CA Leiden, The Netherlands, koehler@strw.leidenuniv.nl*.

We present mid-infrared interferometric observations of the Herbig Ae star R CrA obtained with MIDI at the VLTI using several projected baselines in the UT2-UT3 configuration. The observations show resolved circumstellar emission in the wavelength range 8-13 μm on a $\sim$6 AU scale with a non-symmetric intensity distribution, providing support for an inclined disk geometry. Visibilities are best fitted using a uniform ring model with outer radius in the range 6-10 AU (45-75 mas at 130 pc). The inclination of the ring with respect to the plane of the sky is found to be $\sim 45^\circ$, consistent with the 40° suggested from near-infrared imaging polarimetry [1]. Preliminary results concerning the simultaneous modeling of both visibilities and spectral energy distribution (SED) are presented.

The presence of circumstellar disks around the intermediate mass ($M \lesssim 5 M_\odot$) Herbig Ae stars is supported by a large body of observational evidence [2] [3]. More specifically, while the observed SED of such stars can be explained by both a disk-like distribution of material (e.g. [4]) and other geometries like envelopes (e.g. [5].), clear evidence for circumstellar disks comes from resolved flattened structures observed by interferometry at millimeter, near-IR and recently also mid-IR wavelengths (e.g. [6] [7] [8].).

R CrA is a bright (100 $L_\odot$) young Herbig A5e star, located at the center of a small cluster (The Coronet [9] [10]) at 130 pc [11]. Several characteristics indicate the presence of a circumstellar disk around R CrA : a flat mid-IR to far-IR/mm SED [3], although most of the mm-excess is actually from the nearby embedded infrared source IRS7 [12] and source confusion in the large IRAS beams might be an issue, a broad silicate emission feature [13], a UX Ori Type [14], a high degree (8%) of optical linear polarisation [15] , the possible association with an extended molecular outflow [16] [17] as well as with several Herbig-Haro systems [18], and a near-infrared reflection nebulosity whose resolved spatial polarization is consistent with a bipolar outflow being truncated by an evacuated spherical cavity [1].

R CrA has been observed with MIDI at the VLTI between 2004 July 8 and 30. We obtained 6 sets of spectrally dispersed (Prism, R=30) visibilities in the spectral range 8-13 μm with the 47 m long northeast UT2-UT3 baseline. Projected baseline lengths and PAs are 27.4 m, 46.6 m, 46.2 m, 45.6 m, 40.1 m, 39.6 m and 63°.6, 30°.5, 9°.4, 43°.4, 55°.6, 56°.1, respectively. The raw visibilities were calibrated by observing the source HD 173484, whose adopted angular size is 3.35 $\pm$0.31 mas. We evaluated the error on the visibilities by comparing the instrumental visibility obtained with different calibrators observed during the same night. This leads to a typical relative uncertainty of 15%, a value we adopt in the following.

We compared the observed visibilities with those derived from a simple geometric disk model chosen to be a uniform ring brightness distribution. The inner radius was fixed to a dust sublimation radius of 0.3 AU, typical for a Herbig AeBe star of that luminosity [19]. Spectrally-dispersed visibilities as measured by MIDI are likely to provide additional information, because of the extended *uv*-coverage. However, one should keep in mind that there is in principle a degeneracy between spatial brightness distribution (morphology) and dust spectral emission features. A fortunate observation, in this respect, is that the ISO-SWS spectra are rather featureless apart from a broad 9.7 μm amorphous silicate feature, i.e. no prominent PAH feature at 8.6 μm and no 11 μm complex feature [13]. This allows us to derive meaningful results by fitting our simple uniform ring model to the observed spectrally-dispersed visibilities. Fig. 1 shows the set of observed spectrally-dispersed visibilities together with the best-fit face-on and inclined ring models. Given the possibility that the observed visibilities may be due to the presence of a close companion (R CrA is flagged in Hipparcos as "stochastic binary" and "suspected nonsingle", see also [20]), we additionally fit a binary model to the complete data set. The fitted wavelength-averaged parameters can be found in Table 1. While we can rule out a binary model with a high degree of confidence, the best agreement with these mid-IR visibility data is found for an inclined uniform ring model. The inclination of the ring with respect to the plane of the sky is $44^\circ\,^{+8}_{-17}$. This is fully consistent with the inclination of the plane (40°) perpendicular to the symmetry axis of the bipolar reflection nebula as suggested from NIR imaging polarimetry [1]. However, the derived position angle of the disk symmetry axis ($62^\circ\,^{+14}_{-7}$) is only marginally consistent with R CrA as the driving source for the extended NE-SW molecular outflow at PA$\sim 30^\circ$ [16] [17]. The same conclusion holds for the direction of the closest HH objects with respect to R CrA [18] (HH 96 : $\sim 38^\circ$, HH 97W : $\sim 34^\circ$, HH 98 : $\sim 33^\circ$, HH 100 : $\sim 34^\circ$, HH 99A : $\sim 51^\circ$, HH 104A : $\sim 95^\circ$).

References : [1] Clark, S., McCall, A., Chrysostomou, A. et al., MNRAS, 319, 337 (2000). [2] Natta, A., Grinin, V., Mannings, V., PP IV, p. 559 (2000). [3] Hillenbrand, L.A., Strom, S.E., Vrba, F.J. et al., ApJ, 397, 613 (1992). [4] Dullemond, C.P., Dominik, C. and Natta, A., ApJ, 560, 957 (2001). [5] Hartmann, L., Kenyon, S.J., Calvet, N., ApJ, 407, 219 (1993). [6] Mannings, V. & Sargent, A.I., ApJ, 490, 792 (1997). [7] Eisner, J.A., Lane, B.F., Hillenbrand, L.A., ApJ, 613, 1049 (2004). [8] Leinert, Ch., Van Boekel, R., Waters, L.B.F.M. et al., A&A 423, 537 (2004). [9] Taylor, K.N.R. & Storey, J.W.V., MNRAS, 209, 5 (1984). [10] Wilking, B., McCaughrean, M., Burton, M.G. et al., AJ, 114, 5 (1997). [11] de Zeeus, P.T., Hoogerwerf, R., de Bruijne, J.H.J., AJ, 117, 354 (1999). [12] Choi, M. & Tatematsu, K., ApJ, 600, L55 (2004). [13] Acke, B. & Van den Ancker, M.E., A&A 426, 151 (2004). [14] Dullemond, C.P., Van den Ancker, M.E., Acke, B. et al., ApJ 594, L47 (2003). [15] Bastien, P., ApJ, 317, 231(1987). [16] Levreault, R.M., ApJSS, 67, 283 (1988). [17] Anderson, I.M., Harju, J., Knee, L.B.G., A&A, 321, 575 (1997). [18] Wang, H., Mundt, R., Henning, T. et al., ApJ, 617, 1191 (2004). [19] Monnier, J.D., Millan-Gabet, R., Billmeier, R. et al., ApJ, 624, 832 (2005). [20] Takami, M., Bailey, J., Chrysostomou, A., A&A, 397, 675 (2003).

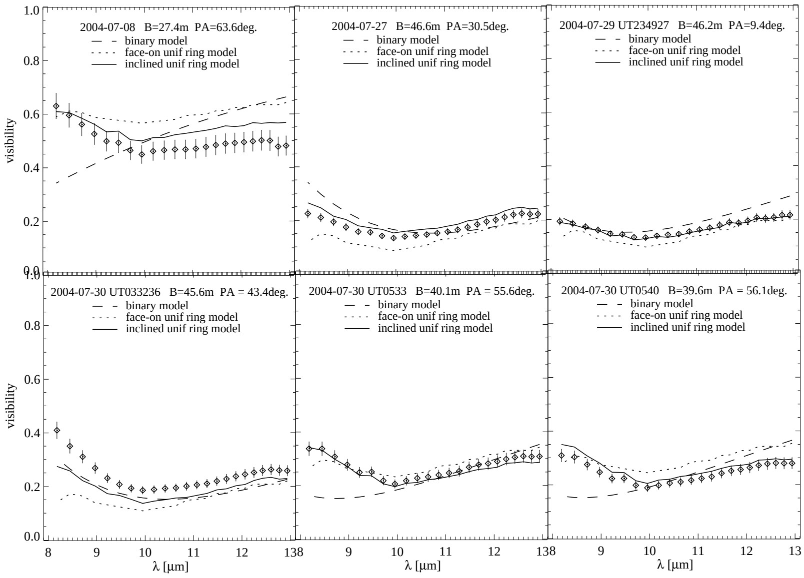

Figure 1: Spectrally-dispersed visibilities between with 8-13 μm (diamonds) with the best-fit models (binary, face-on and inclined uniform rings).

Table 1: Best-fit models based on spectrally-dispersed visibilities. Uniform ring parameters are wavelength-averaged values. The binary model separation, brightness ratio and PA are quoted in the R_{out}, i and PA columns, respectively.

	reduced χ^2	R_{out} (AU)	i (°)	PA (°)
Binary	2.4	$3.1^{+0.2}_{-0.2}$	$0.44^{+0.05}_{-0.04}$	36^{+10}_{-10}
Face-on uniform ring	2.2±0.7	$6.43^{+0.15}_{-0.15}$	...	...
Inclined uniform ring	1.3±0.6	$8.48^{+1.26}_{-1.47}$	44^{+8}_{-17}	152^{+14}_{-7}

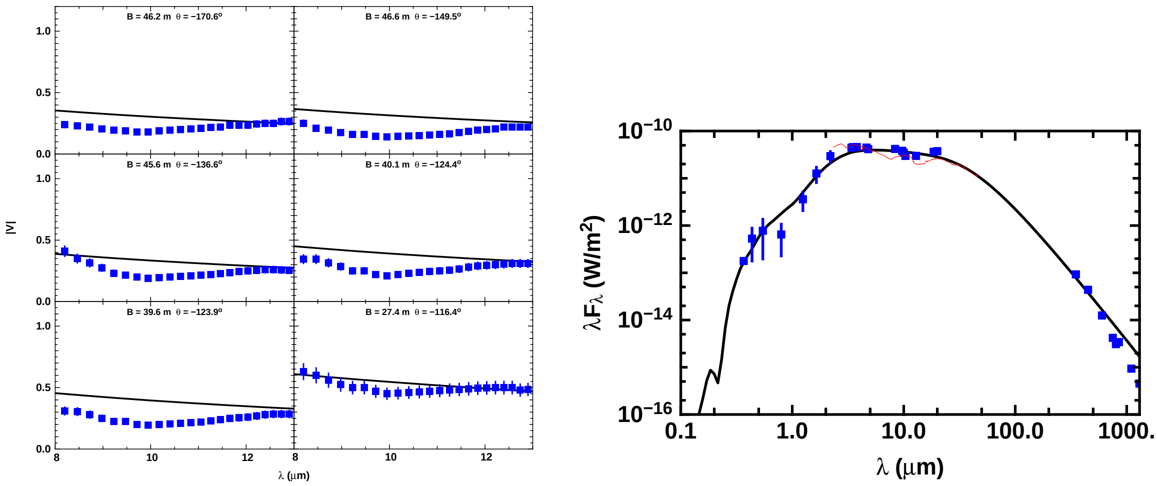

Figure 2: Simultaneous fit of the visibilities (left) and SED (right). The best fit model shown is composed of the star (R=1.8 $R_\odot$, $T_{\rm eff}$=7500 K), an accretion disk (power-law temperature profile index 0.55, T(1AU)=650 K, minimum radius 0.16 AU, maximum radius 30 AU, inclination 30 deg., PA -10 deg.) and an inner ring (radius 0.12 AU, width 0.05 AU, temperature 1500 K, same inclination and PA). We assumed A_v=3 mag and a distance of 130 pc. Squares are measurements, while the continuous line is the best fit model. The red line is the ISO spectrum.